

# Preclinical evaluation of therapeutic vaccines for chronic hepatitis B that stimulate antiviral activities of T cells and NKT cells

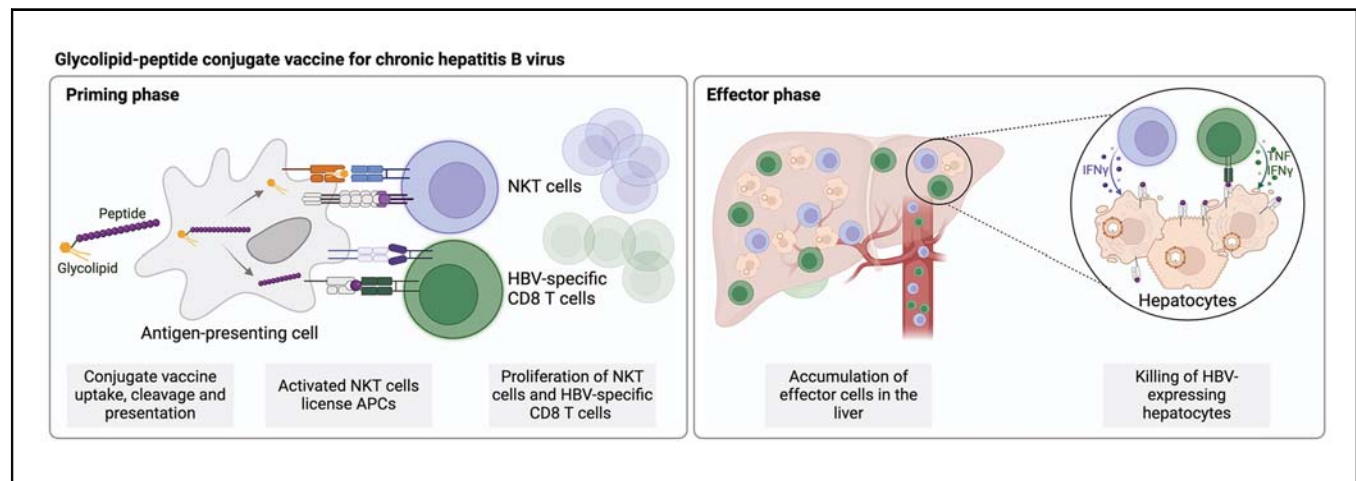
## Authors

Anna H. Mooney, Sarah L. Draper, Olivia K. Burn, Regan J. Anderson, Benjamin J. Compton, Chingwen Tang, Kathryn J. Farrand, Pietro Di Lucia, Micol Ravà, Valeria Fumagalli, Leonardo Giustini, Elisa Bono, Dale I. Godfrey, William R. Heath, Weiming Yuan, Francis V. Chisari, Luca G. Guidotti, Matteo Iannacone, John Sidney, Alessandro Sette, Shivali A. Gulab, Gavin F. Painter, Ian F. Hermans

## Correspondence

[gavin.painter@vuw.ac.nz](mailto:gavin.painter@vuw.ac.nz) (G.F. Painter), [ihermans@malaghan.org.nz](mailto:ihermans@malaghan.org.nz) (I.F. Hermans).

## Graphical abstract



## Highlights

- Type I natural killer T (NKT) cells have antiviral activity against HBV and can also function as helper cells.
- Vaccines prepared by conjugating T-cell epitopes from viral antigens to an NKT cell agonist were shown to be immunogenic.
- Vaccines reduce virus levels in a mouse model of chronic hepatitis B.
- Vaccines prepared using long peptides covering clusters of known HLA-binding virus epitopes were shown to be immunogenic.

## Impact and Implications

Although there are effective prophylactic vaccines for HBV infection, it is estimated that 350–400 million people worldwide have chronic hepatitis B, putting these individuals at significant risk of life-threatening liver diseases. Therapeutic vaccination aimed at activating or boosting HBV-specific T-cell responses holds potential as a strategy for treating chronic infection, but has so far met with limited success. Here, we show that a glycolipid-peptide conjugate vaccine designed to coordinate activity of type I NKT cells alongside conventional antiviral T cells has antiviral activity in a mouse model of chronic infection. It is anticipated that a product based on a combination of three such conjugates, each prepared using long peptides covering clusters of known HLA-binding epitopes, could be developed further as a treatment for chronic hepatitis B with broad global HLA coverage.

# Preclinical evaluation of therapeutic vaccines for chronic hepatitis B that stimulate antiviral activities of T cells and NKT cells



Anna H. Mooney,<sup>1</sup> Sarah L. Draper,<sup>2</sup> Olivia K. Burn,<sup>1</sup> Regan J. Anderson,<sup>2</sup> Benjamin J. Compton,<sup>2</sup> Chingwen Tang,<sup>1</sup> Kathryn J. Farrand,<sup>1</sup> Pietro Di Lucia,<sup>3,4</sup> Micol Ravà,<sup>3,4</sup> Valeria Fumagalli,<sup>3,4</sup> Leonardo Giustini,<sup>3</sup> Elisa Bono,<sup>3</sup> Dale I. Godfrey,<sup>5,6</sup> William R. Heath,<sup>5</sup> Weiming Yuan,<sup>7</sup> Francis V. Chisari,<sup>8</sup> Luca G. Guidotti,<sup>3,4</sup> Matteo Iannacone,<sup>3,4</sup> John Sidney,<sup>9</sup> Alessandro Sette,<sup>9</sup> Shivali A. Gulab,<sup>2,10</sup> Gavin F. Painter,<sup>2,\*</sup> Ian F. Hermans<sup>1,\*</sup>

<sup>1</sup>Malaghan Institute of Medical Research, Wellington, New Zealand; <sup>2</sup>Ferrier Research Institute, Victoria University of Wellington, Wellington, New Zealand; <sup>3</sup>Division of Immunology, Transplantation and Infectious Diseases, IRCCS San Raffaele Scientific Institute, Milan, Italy; <sup>4</sup>Vita-Salute San Raffaele University, Milan, Italy; <sup>5</sup>Department of Microbiology and Immunology, Peter Doherty Institute for Infection and Immunity, University of Melbourne, Victoria, Australia; <sup>6</sup>Australian Research Council Centre of Excellence in Advanced Molecular Imaging, University of Melbourne, Parkville, Australia; <sup>7</sup>Department of Molecular Microbiology and Immunology, Keck School of Medicine, University of Southern California, Los Angeles, CA, USA; <sup>8</sup>Department of Immunology & Microbial Sciences, The Scripps Research Institute, La Jolla, CA, USA; <sup>9</sup>Center for Infectious Disease and Vaccine Research, La Jolla Institute for Immunology, La Jolla, CA, USA; <sup>10</sup>Avalia Immunotherapies Limited, Wellington, New Zealand

JHEP Reports 2024. <https://doi.org/10.1016/j.jhepr.2024.101038>

**Background & Aims:** Liver diseases resulting from chronic HBV infection are a significant cause of morbidity and mortality. Vaccines that elicit T-cell responses capable of controlling the virus represent a treatment strategy with potential for long-term effects. Here, we evaluated vaccines that induce the activity of type I natural killer T (NKT) cells to limit viral replication and license stimulation of conventional antiviral T-cells.

**Methods:** Vaccines were prepared by conjugating peptide epitopes to an NKT-cell agonist to promote co-delivery to antigen-presenting cells, encouraging NKT-cell licensing and stimulation of T cells. Activity of the conjugate vaccines was assessed in transgenic mice expressing the complete HBV genome, administered intravenously to maximise access to NKT cell-rich tissues.

**Results:** The vaccines induced only limited antiviral activity in unmanipulated transgenic hosts, likely attributable to NKT-cell activation as T-cell tolerance to viral antigens is strong. However, in a model of chronic hepatitis B involving transfer of naive HBcAg-specific CD8<sup>+</sup> T cells into the transgenic mice, which typically results in specific T-cell dysfunction without virus control, vaccines containing the targeted HBcAg epitope induced prolonged antiviral activity because of qualitatively improved T-cell stimulation. In a step towards a clinical product, vaccines were prepared using synthetic long peptides covering clusters of known HLA-binding epitopes and shown to be immunogenic in HLA transgenic mice. Predictions based on HLA distribution suggest a product containing three selected SLP-based vaccines could give >90 % worldwide coverage, with an average of 3.38 epitopes targeted per individual.

**Conclusions:** The novel vaccines described show promise for further clinical development as a treatment for chronic hepatitis B.

**Impact and Implications:** Although there are effective prophylactic vaccines for HBV infection, it is estimated that 350–400 million people worldwide have chronic hepatitis B, putting these individuals at significant risk of life-threatening liver diseases. Therapeutic vaccination aimed at activating or boosting HBV-specific T-cell responses holds potential as a strategy for treating chronic infection, but has so far met with limited success. Here, we show that a glycolipid-peptide conjugate vaccine designed to coordinate activity of type I NKT cells alongside conventional antiviral T cells has antiviral activity in a mouse model of chronic infection. It is anticipated that a product based on a combination of three such conjugates, each prepared using long peptides covering clusters of known HLA-binding epitopes, could be developed further as a treatment for chronic hepatitis B with broad global HLA coverage.

© 2024 The Authors. Published by Elsevier B.V. on behalf of European Association for the Study of the Liver (EASL). This is an open access article under the CC BY-NC-ND license (<http://creativecommons.org/licenses/by-nc-nd/4.0/>).

Keywords: Hepatitis B virus; Glycolipid peptide conjugate vaccine; Natural killer T cells; Synthetic long peptide.

Received 6 September 2023; received in revised form 1 February 2024; accepted 6 February 2024; available online 12 February 2024

\* Corresponding authors. Addresses: Ferrier Research Institute, Victoria University of Wellington, PO Box 33436, Wellington 5046, New Zealand. Tel.: +6444630058 (G.F. Painter); Malaghan Institute of Medical Research, PO Box 7060, Wellington 6242, New Zealand. Tel.: +6444996914 (I.F. Hermans).

E-mail addresses: [gavin.painter@vuw.ac.nz](mailto:gavin.painter@vuw.ac.nz) (G.F. Painter), [ihermans@malaghan.org.nz](mailto:ihermans@malaghan.org.nz) (I.F. Hermans).



## Introduction

Hepatitis B is caused by HBV, a non-cytopathic double-stranded DNA virus that specifically infects hepatocytes and is transmitted by contact with infected blood and body fluids. Although most adults can resolve acute HBV infection, perinatally infected infants and approximately 5% of untreated adults develop chronic infection. In fact, the global prevalence of chronic hepatitis exceeds 250 million individuals. Chronic HBV carriers are at increased risk of developing cirrhosis, a late-stage condition characterised by irreversible liver scarring, which can progress to liver failure and liver cancer.<sup>1,2</sup>

The standard treatment for chronic hepatitis B involves nucleoside/nucleotide inhibitors (entecavir and tenofovir) that incorporate into growing viral DNA strands, inhibiting the activity of viral DNA polymerase. However, complete viral elimination is rare, and patients typically require lifelong treatment and monitoring at a high cost. Pegylated interferon (IFN)- $\alpha$  can achieve sustained off-treatment control but is effective in only a limited proportion of patients.<sup>3,4</sup> Furthermore, despite available treatments, the majority of HBV carriers worldwide remain untreated. This is primarily because of inadequate health infrastructure in endemic countries and the financial and logistical burdens associated with regular screening.<sup>5–7</sup> There is therefore a need for new therapies for chronic hepatitis B. The challenge is to achieve a sustained functional cure, characterised by undetectable levels of circulating HBsAg and HBV DNA, absence of liver injury, and the presence of antiviral antibodies (anti-HBs) – a state that is similar to that of individuals who successfully resolve acute HBV infection. Although complete eradication of the virus may be challenging, therapies that stably maintain low levels of HBV replication under the control of a functional antiviral immune response may be attainable.

Studies conducted in chimpanzees have shown that CD8<sup>+</sup> effector T cells play a critical role in clearing HBV during acute infection.<sup>8</sup> Furthermore, individuals with chronic disease have been able to resolve the infection following bone marrow or liver transplantation from donors that have pre-existing HBV immunity,<sup>9–12</sup> highlighting a potentially powerful role for adaptive immunity in this setting as well. However, the development of chronic hepatitis B is typically associated with progressive inability to induce or maintain functional virus-specific T cells. Although T-cell responses in acute infection are robust and broad, targeting the range of viral proteins, T-cell responses in chronically infected patients are generally weak and limited in their specificity.<sup>13</sup> Increasing evidence suggests CD4<sup>+</sup> T cells are also essential in viral clearance, particularly as helper cells to support CD8<sup>+</sup> T cells and antibody responses.<sup>14–16</sup> Therefore, therapeutic vaccination aimed at activating or boosting HBV-specific T-cell responses holds potential as a therapeutic strategy for treating chronic HBV infection. However, such approaches have so far met with limited success.<sup>17</sup> This is attributable to T-cell tolerance mechanisms, likely driven by preferential expression of viral antigens by hepatocytes rather than by professional antigen-presenting cells, such as dendritic cells (DCs), together with an abundance of viral antigens that can lead to T-cell deletion or exhaustion.<sup>18,19</sup>

Unconventional T cells, characterised by restricted T-cell receptor (TCR) usage and selection via non-polymorphic antigen-presenting molecules, can differentiate into polarised effector cells with properties similar to those of specialised CD4<sup>+</sup> T-cell subsets.<sup>20</sup> The liver is a rich source of these cells, notably

mucosal-associated invariant T (MAIT) cells, and type I natural killer T (NKT) cells. The latter, recognising lipid-based antigens presented on CD1d molecules,<sup>21</sup> have been implicated in the control of HBV in a mouse model of chronic infection,<sup>22</sup> triggered by injection of the specific NKT-cell agonist  $\alpha$ -galactosylceramide ( $\alpha$ -GalCer).<sup>23</sup> Although significant IFN- $\gamma$ -mediated inhibition of HBV replication is observed, the effect is only transient. Administration of  $\alpha$ -GalCer to patients with HBV infection in the clinic has also been shown to lack clinical efficacy.<sup>24</sup> However, it is important to note that NKT cells can serve additional functions, notably as helper cells to support CD8<sup>+</sup> T cells and antibody responses through their ability to activate antigen-presenting cells.<sup>25</sup> This relies on the co-ordinated presentation of NKT-cell agonists and protein antigens in the lymphoid tissues. Ideally, antigen-presenting cells are initially 'conditioned' through interaction with NKT cells, and then these same cells present processed antigen in a highly stimulatory manner to T cells to promote strong antigen-specific responses, a process analogous to CD4<sup>+</sup> T cell helper function. To harness the full potential of NKT-cell activation in control of HBV, it may be possible to exploit their direct antiviral effector activities within the liver alongside their helper properties.

Here, we describe a synthetic vaccine platform in which major histocompatibility complex (MHC)-binding antigenic peptides from HBV proteins are attached directly to a derivative of  $\alpha$ -GalCer, with the aim of promoting co-delivery of NKT-cell agonist and viral antigens to the same antigen-presenting cells *in vivo*. Once acquired, the active form of  $\alpha$ -GalCer is released from the peptide and both components enter their respective antigen-presentation pathways. This vaccine design effectively activates NKT cells and stimulates HBV-specific IFN- $\gamma$ -secreting CD8<sup>+</sup> T cells, leading to improved viral clearance in an HBV transgenic mouse model of chronic hepatitis B. To advance this vaccine platform for clinical use, we prepared conjugates using synthetic long peptides (SLPs) containing clusters of HBV epitopes to take into account human leukocyte antigen (HLA) diversity in the human population and showed that these vaccines exhibited activity in HLA transgenic mice.

## Materials and methods

### Ethics approval

Experiments in Figs 1 and 4 were performed at the Malaghan Institute of Medical Research, Wellington, New Zealand in accordance with the Animal Welfare Act of New Zealand (1999) using protocols AEC23784, AEC23803, AEC26384, AEC28165 approved by the Victoria University Animal Ethics Committee, Wellington, New Zealand. Experiments in Figs 2 and 3 were performed at the San Raffaele Scientific Institute, Milan, Italy. All experimental animal procedures were approved by the Institutional Animal Committee of the San Raffaele Scientific Institute, Milan, Italy.

### Mice

Mice were sex-matched and used between 5 and 12 weeks of age; experiments were conducted under pathogen-free conditions with mice randomly assigned to experimental groups. Strains used were: C57BL/6J mice (Jackson Laboratories, Bar Harbor, ME, USA); *Traj18*<sup>-/-</sup> mice, which are devoid of type I NKT cells (Jackson Laboratories);<sup>26</sup> C57BL/6J-TgN(A2KbHLA) 6HsdArc (*HLA-A2-K<sup>b</sup>* transgenic mice)<sup>27</sup> (Animal Resource

Centre, WA, Australia); human CD1d-knock-in (*hCD1d-KI* mice), in which the murine CD1 gene is replaced by the human CD1d gene;<sup>28</sup> D<sub>H</sub>LMP2A mice,<sup>29</sup> which cannot produce surface-expressed and secreted antibodies (originally provided by K. Rajewsky, Harvard Medical School, Boston, MA, USA); 1.3.32 lineage HBV transgenic mice (*HBV Tg*), which express all HBV antigens and replicate HBV in the liver at high levels without evidence of cytopathology;<sup>30</sup> and BC10.3 (inbred CD45.1) mice, which express V $\alpha$ 13.1J $\alpha$ NEW06 and V $\beta$ 8.1J $\beta$ 1.2 transgenes, resulting in >98% of naive splenic CD8<sup>+</sup> T cells recognising the H-2K<sup>b</sup>-restricted epitope HBcAg<sub>93-100</sub> (HBcAg<sub>93-100</sub> T<sub>N</sub> cells).<sup>31</sup> Studies of antiviral activity of the vaccines were conducted under BSL-3 barrier conditions, using hosts from a cross of HBV Tg mice and D<sub>H</sub>LMP2a mice to avoid confounding antibody mediated activity.

### Preparation of glycolipids and glycolipid-peptide conjugate vaccines

The NKT-cell agonist  $\alpha$ -GalCer was manufactured in-house.<sup>32</sup> Solubilisation was achieved by freeze-drying in the presence of sucrose, L-histidine, and Tween 20,<sup>33</sup> and resuspending in sterile injection water to give a stock concentration of 582  $\mu$ M; this was further diluted in PBS to give the required dose for i.v. injection. The glycolipid-peptide conjugate vaccines were prepared using an inactive derivative of  $\alpha$ -GalCer with an intramolecular N $\rightarrow$ O migration of the acyl group<sup>34</sup> that permitted the peptide to be conjugated via a valine-citrulline-*p*-amino-benzyl carbamate linker to the exposed amino group. The glycolipid reverts to the active N-acyl form under physiological conditions following cathepsin-mediated release of the attached peptide and immolation of the linker.<sup>35</sup> The proteolytic site FFRK was added to the N-terminus of attached peptides to ensure release of incorporated antigen-specific peptide sequences<sup>36</sup> except for the HBcAg peptide where the FFRK was omitted and replaced with natural flanking residues for solubility purposes. The final peptide sequences were modified with amino-oxyacetic acid (AoAA) at the N-terminus to facilitate oxime ligation with the ketone group of the linker for conjugation. Four vaccines were prepared with defined H-2K<sup>b</sup>-binding epitopes from HBV antigens: three from HBsAg ( $\alpha$ -GalCer-HBsAg<sub>179-186</sub>, FVQWVGL;  $\alpha$ -GalCer-HBsAg<sub>353-360</sub>, VWLSVIWM;  $\alpha$ -GalCer-HBsAg<sub>371-378</sub>, IILSPFLPL), and one from HBcAg ( $\alpha$ -GalCer-HBcAg<sub>93-100</sub> with additional flanking regions from the protein sequence, NTN-MGLKFRQL-LWF). A control vaccine with irrelevant peptide was prepared with the H-2K<sup>b</sup>-binding epitope from chicken ovalbumin (OVA) ( $\alpha$ -GalCer-OVA<sub>257-264</sub>; SIINFEKL). Three additional HBV-targeting vaccines were prepared with longer peptides encoding clusters of overlapping HLA-binding epitopes defined as described in the text: two from HBcAg/HBeAg ( $\alpha$ -GalCer-HBV<sub>cluster1</sub>, LSFPSDFPFSVRDLLDTASALY) and  $\alpha$ -GalCer-HBV<sub>cluster3</sub>, YVNTNMGLKILQLLWFHISCLTFGRETVLEN), and one from Pol ( $\alpha$ -GalCer-HBV<sub>cluster28</sub>, QAFTFSPTYKAFKQQYMNL). The vaccines were lyophilised in the presence of solubilisation matrix, as for  $\alpha$ -GalCer above, resuspended to 0.5 mg/ml in sterile injection water, and diluted in PBS to the desired concentration for i.v. injection. All injected vaccines had endotoxin levels below the recommended limit of 0.75 EU/ml<sup>37</sup> (Pierce Chromogenic Endotoxin Quant Kit). Synthesis and characterisation of peptides and vaccines are described in more detail in the Supplementary Methods. For i.v. administration, a 200  $\mu$ l volume was injected via the lateral vein in a slow continuous stream using an Ultra-Fine 1 ml 27 G syringe (BD; Franklin Lakes, NJ, USA). Doses are specified in the figure legends.

### Epitope identification for SLP design

The Immune Epitope Database (IEDB) ([www.iedb.org](http://www.iedb.org)) was queried for linear peptide sequences derived from HBV (organism ID 10407), with humans specified as the host organism (taxonomy organism ID 9606), with each peptide reported to elicit immune responses restricted by human class I HLA molecules; data generated in HLA transgenic mice were also included. Initially, 177 unique epitopes associated with 901 assays from 118 references were identified. Of these, 91 epitopes were excluded as they did not meet the desired characteristics (size and/or characterisation was limited to a single assay). The remaining set of 86 HBV-derived HLA class I-restricted T-cell epitopes, representing 114 different HLA restrictions was further analysed (Table S1). Proto-clusters of overlapping or nested sequences were identified and expanded to incorporate additional epitopes in both the N- and C-terminal directions until spans of up to approximately 32 residues were selected. In most cases, breaks between epitope groups were readily apparent, such that natural clusters were easily parsed out. In the few cases where contiguous stretches of epitopes could be identified that extended beyond 32 residues, breaks were made to the two most dominant clusters in terms of breadth of coverage (where population coverage is defined as the percentage of individuals that express at least one of the HLA A or B alleles known to restrict the selected epitopes).

### Processing tissues

Mice were sacrificed by CO<sub>2</sub> asphyxiation to harvest tissues. Spleens were processed to a single cell suspension by washing through a 70  $\mu$ m cell strainer with Roswell Park Memorial Institute (RPMI) medium (Gibco). After centrifugation at 1,503  $\times$  g for 4 min, red blood cells (RBCs) were lysed with 2 ml RBC lysis buffer (Qiagen, CA, USA) for 2 min at room temperature (RT), followed by centrifugation and resuspension of the pellet in FACS buffer (PBS supplemented with 1% FBS, 0.0001% Na<sub>3</sub>, and 2 mM EDTA) for flow cytometry, or complete RPMI (10% FBS, 1% penicillin-streptomycin, 0.5% 2-mercaptoethanol; all Gibco) for ELISpot analysis. Livers samples were processed to a single cell suspension by washing through a 70  $\mu$ m cell strainer with PBS and centrifuged at 1,503  $\times$  g for 4 min. Cells were then resuspended in 10 ml of 33% Percoll (Cytiva, Uppsala, Sweden) in PBS with 2% Asever's solution (Sigma, UK) and centrifuged at 670  $\times$  g for 20 min with no deceleration. The cell pellet was washed with RPMI and centrifuged at 1,503  $\times$  g for 4 min before decanting the supernatant and lysing RBCs with 5 ml RBC lysis buffer for 5 min at 37  $^{\circ}$ C. The wash and centrifuge steps were repeated, and cells resuspended in complete RPMI or FACS buffer for further use.

### ELISpot assays

Peptide-specific T-cell responses were determined using a mouse IFN- $\gamma$  ELISpot kit (Mabtech AB, Sweden) according to the manufacturer's protocol. Briefly, 96-well filter plates pre-coated in the IFN- $\gamma$  monoclonal antibody (mAb) were washed with PBS then blocked for 2 h at RT with complete RPMI. Single-cell suspensions from processed tissues were seeded at 3  $\times$  10<sup>5</sup> live cells/well and incubated with the relevant peptides (10  $\mu$ M final solution), or no peptide, for 16 h at 37  $^{\circ}$ C. Cells stimulated with 2.5 ng/ml phorbol 12-myristate 13-acetate and 1 ng/ml ionomycin served as a positive control for cytokine induction. Cells were then washed with PBS and incubated with 100  $\mu$ l biotinylated anti-mouse IFN- $\gamma$  antibody (1:1,000) diluted in 0.05%

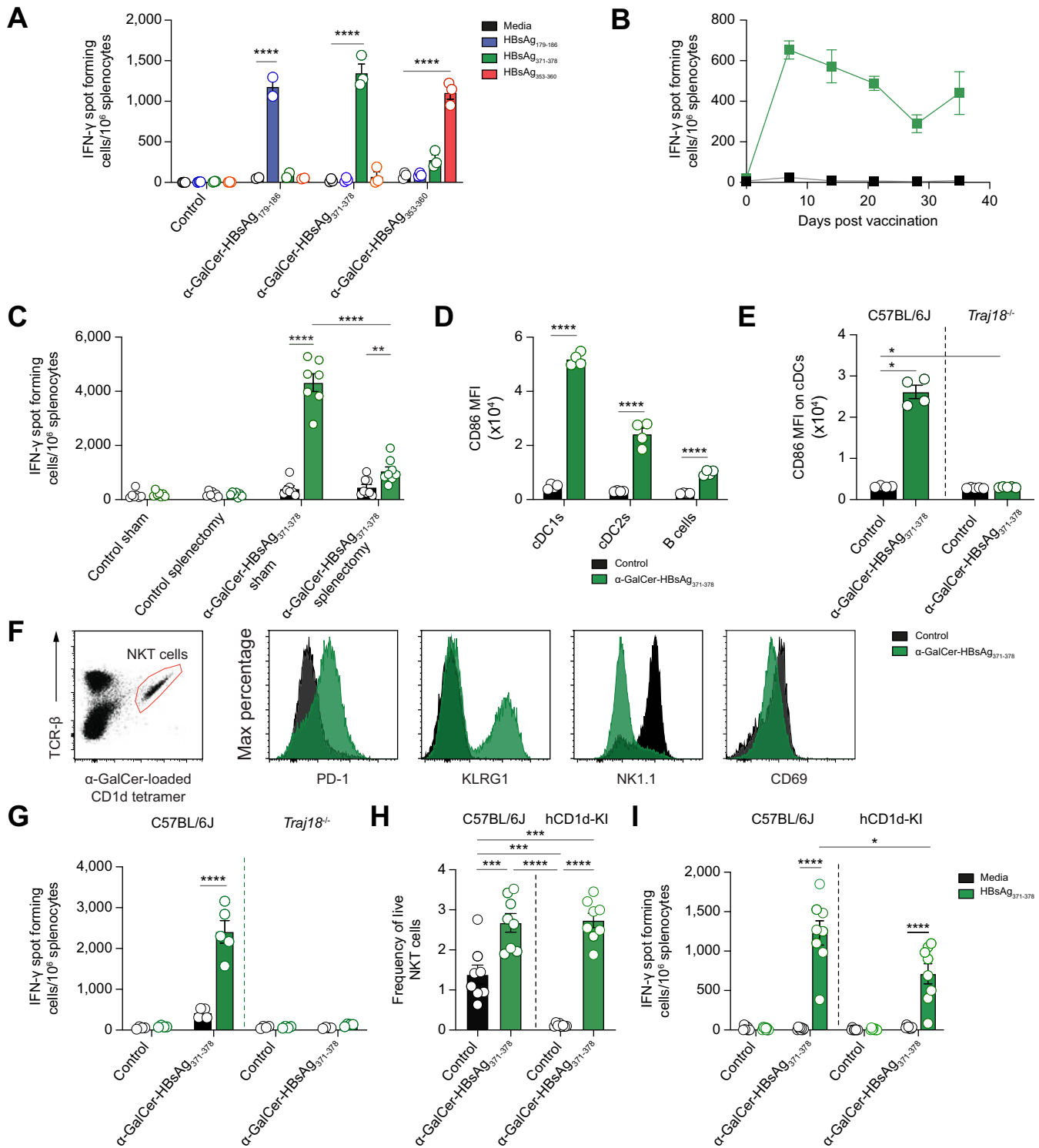


**Fig. 1. Conjugate vaccines stimulate NKT cells and HBV antigen-specific T cells.** (A) Wild-type (C57BL/6J) mice ( $n = 3$ ) were vaccinated intravenously with a single 1 nmol dose of  $\alpha$ -GalCer-HBsAg<sub>179-186</sub>,  $\alpha$ -GalCer-HBsAg<sub>371-378</sub> or  $\alpha$ -GalCer-HBsAg<sub>353-360</sub>, or with PBS as control. Seven days later splenocytes were harvested for analysis of vaccine-specific T-cell responses by IFN- $\gamma$  ELISpot following restimulation on minimal H-2K<sup>b</sup>-binding peptides from HBsAg. Mean spot forming units (SFU)  $\pm$  SEM for each group are shown; each symbol represents an individual mouse. \*\* $p < 0.01$ , \*\*\* $p < 0.001$ , \*\*\*\* $p < 0.0001$ ; two-way ANOVA followed by Tukey's multiple comparison test. Data are representative of at least two experiments conducted per vaccine. (B) Time course of response to  $\alpha$ -GalCer-HBsAg<sub>371-378</sub> ( $n = 3$  per timepoint). (C) Mice ( $n = 7-8$ ) were subjected to splenectomy, or sham surgery, and then rested for 21 days before being vaccinated with  $\alpha$ -GalCer-HBsAg<sub>371-378</sub>. Analysis of T-cell response was conducted by ELISpot on liver cells 7 days later. \*\* $p < 0.01$ , \*\*\* $p < 0.001$ , \*\*\*\* $p < 0.0001$ ; two-way ANOVA followed by Tukey's multiple comparison test. Data are representative of two experiments. (D) Expression of CD86 on splenic cDC1, cDC2 and B cells 18 h after vaccine or PBS control ( $n = 4-5$ ). Gating strategy is shown in Fig. S2. \*\*\*\* $p < 0.0001$ ; Unpaired t-test. (E) CD86 expression on all DCs (CD11c<sup>+</sup> cells) 18 h after vaccination in wild-type vs. *Tra18<sup>-/-</sup>* mice ( $n = 5$ ). \* $p < 0.05$ ; one-way ANOVA followed by Tukey's multiple comparison test. (F) Representative flow plots for analysis of NKT cells. Gating strategy and quantification of the NKT-cell phenotypic markers is shown in Fig. S3. (G) ELISpot analysis of splenocytes from wild-type vs. *Tra18<sup>-/-</sup>* mice 7

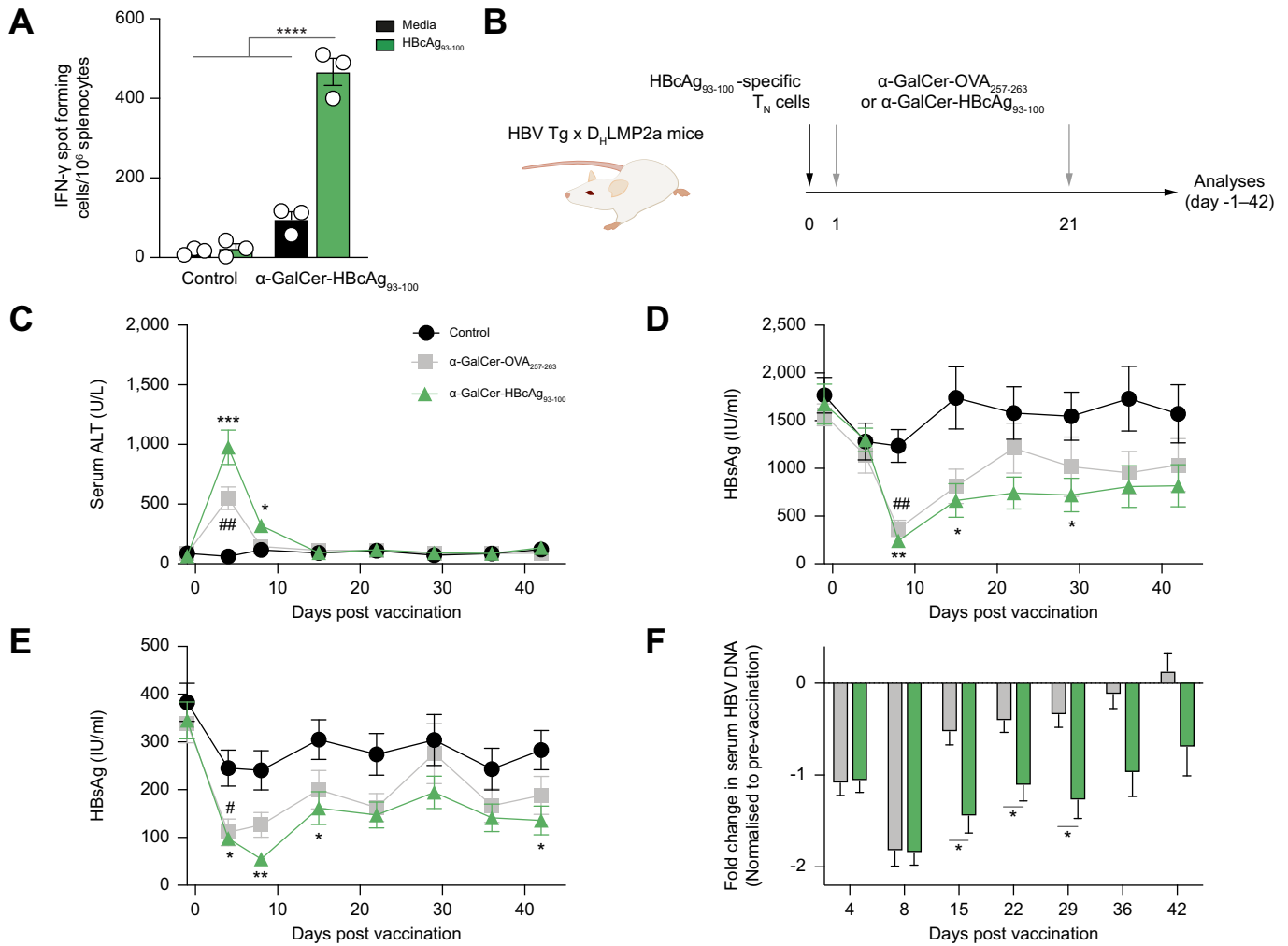


**Fig. 2. Vaccination in HBV transgenic mice.** (A) Evaluation of  $\alpha$ -GalCer-HBcAg<sub>93-100</sub> vaccine in C57BL/6 mice. IFN- $\gamma$  ELISpot analysis of splenocytes 7 days after injection with 1 nmol vaccine or PBS control ( $n = 3$ ). \*\*\*\* $p < 0.0001$ ; two-way ANOVA test with Tukey's multiple comparison test. (B) Schematic representation of the experimental set-up in groups of HBV Tg  $\times$  D<sub>H</sub>LMP2a mice ( $n = 8$ ). A day before vaccination with  $\alpha$ -GalCer-HBcAg<sub>93-100</sub> or  $\alpha$ -GalCer-OVA<sub>257-264</sub>, animals received  $10^6$  naive HBcAg<sub>93-100</sub>-specific CD8<sup>+</sup> T cells intravenously; the vaccines were administered again 21 days later. The control group received no transgenic T cells, with NaCl administered at the times of injection in experimental groups. (C) Serum ALT concentrations over time. (D) Serum HBsAg titres. (E) Serum HBeAg titres. (F) Serum HBV DNA levels expressed as fold reduction over pre-vaccination values. Data for C–F are all expressed as mean  $\pm$  SEM. \* $p < 0.05$ , \*\* $p < 0.01$ , \*\*\* $p < 0.001$ , \*\*\*\* $p < 0.0001$  refer to comparison of  $\alpha$ -GalCer-HBcAg<sub>93-100</sub> group to control; # $p < 0.05$ , ### $p < 0.01$  to comparison of  $\alpha$ -GalCer-OVA<sub>257-264</sub> to control; two-way ANOVA with Tukey's multiple comparison test. ALT, alanine transferase.

foetal calf serum in PBS for 2 h at RT. Following a further wash step, 100  $\mu$ l streptavidin-alkaline phosphatase (ALP; 1:1,000) was added to each well for 1 h at RT. The plate was then washed and developed with 5-bromo-4-chloro-3-indolyl phosphate/nitro blue tetrazolium-plus substrate until all spots were clearly visible. Plates were then washed extensively in tap water and spot-forming cells were counted with an AID 5,000 pro XI ELISpot reader (Autoimmun Diagnostika, Strassberg, Germany).

### Flow cytometry

Cells were plated at  $\sim 2 \times 10^6$  cells per well in a 96-well plate, centrifuged at 800  $\times$  g for 2 min and the supernatant removed.

Non-specific FcR-mediated Ab staining was blocked by incubation with 50  $\mu$ l anti-CD16/32 antibody (24G2; 1:100) in FACS buffer for 10 min at RT. Cells were washed in 150  $\mu$ l FACS buffer, centrifuged and the supernatant discarded. To enable gating of viable cells 50  $\mu$ l Live/Dead Zombie NIR dye (Biolegend, CA, USA) in PBS was added for 15 min at RT. Cells were washed in 150  $\mu$ l FACS buffer, centrifuged as above and the supernatant discarded. Cells were then labelled with 50  $\mu$ l of antibody staining panel made up in FACS buffer (antibody panels are provided in [Tables S3 and S4](#)). All antibody and tetramer optimal concentrations used were previously established by titrations on splenocytes. Note that NKT cells were detected using CD1d tetramers that

days after vaccine or PBS ( $n = 5$ ). Mean SFU  $\pm$  SEM for each group are shown; each symbol represents an individual mouse. \*\*\*\* $p < 0.001$ ; one-way ANOVA followed by Tukey's multiple comparison test. (H) Frequency of NKT cells in spleens of wild-type vs. hCD1d-KI mice 7 days after vaccine or PBS ( $n = 3$ ). \*\* $p < 0.01$ , \*\*\* $p < 0.001$ , \*\*\*\* $p < 0.0001$ ; one-way ANOVA followed by Tukey's multiple comparison test. Data are representative of two experiments. (I) ELISpot analysis of splenocytes from wild-type vs. hCD1d-KI mice 7 days after vaccine or PBS ( $n = 3$ ). \* $p < 0.05$ , \*\*\*\* $p < 0.0001$ ; two-way ANOVA followed by Tukey's multiple comparison test. Data are representative of two independent experiments.

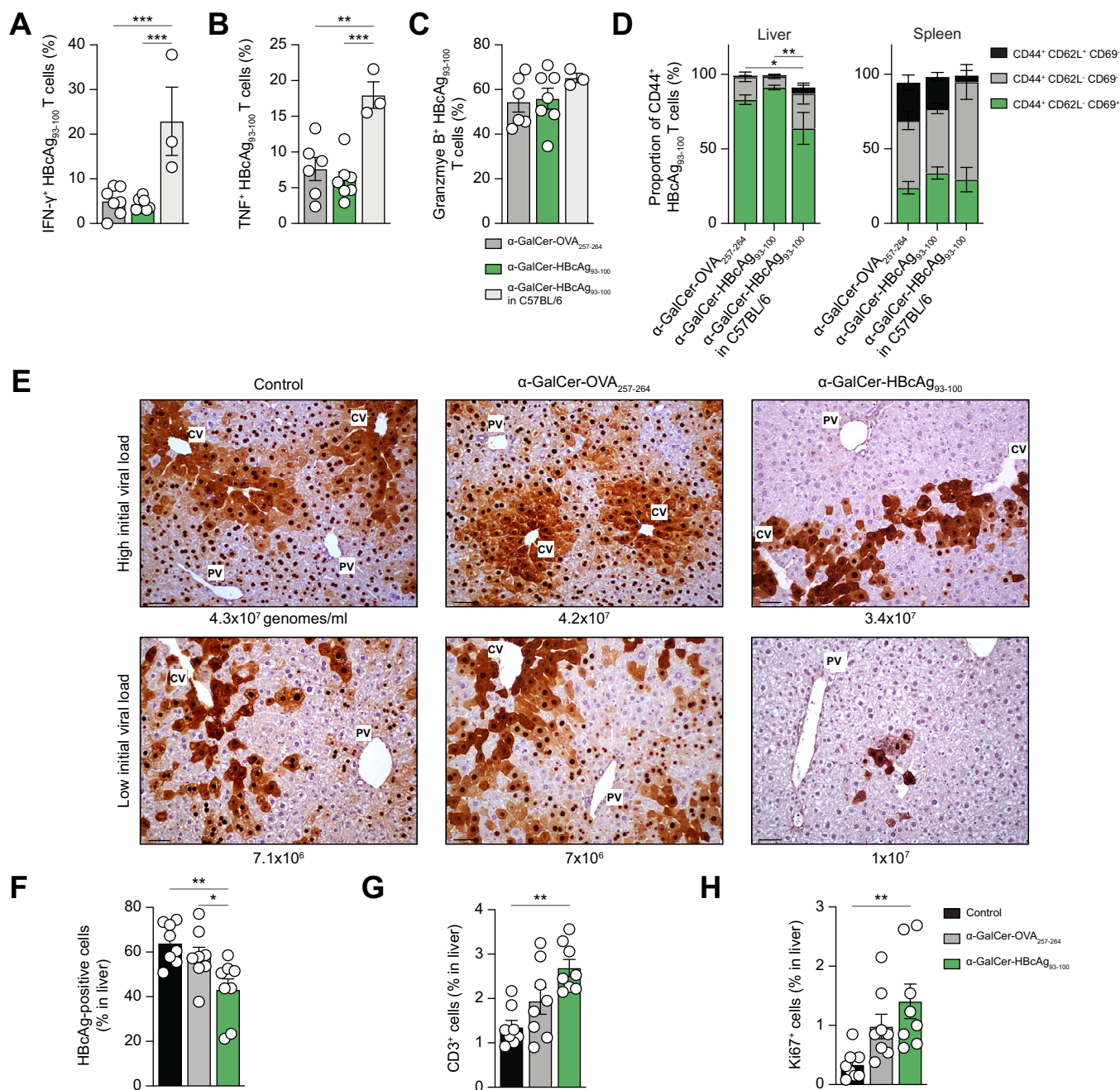


**Fig. 3. Flow cytometry and immunohistochemistry after vaccination.** Further to the experimental set-up in Fig. 2B–F, an additional group of C57BL/6 mice ( $n = 6$ ) received naive HBcAg<sub>93-100</sub>-specific CD8<sup>+</sup> T cells and was vaccinated with the same dose and schedule with  $\alpha$ -GalCer-HBcAg<sub>93-100</sub> vaccine. Livers and spleen were collected from all vaccinated groups at the end of the experiment for flow cytometry. (A–C) Mean frequency  $\pm$  SEM of activated transgenic T cells expressing IFN- $\gamma$ , TNF, or granzyme B for indicated treatment groups as determined by flow cytometry using the gating strategy shown in Fig. S3, conducted on animals with sufficient evaluable material. Individual mice are indicated by symbols. \*\* $p < 0.01$ , \*\*\* $p < 0.001$ ; one-way ANOVA test with Tukey’s multiple comparison test. (D) Proportions of activated transgenic T cells defined as resident memory ( $T_{RM}$ ), central memory ( $T_{CM}$ ) or effector memory ( $T_{EM}$ ) T cells using the gating strategy shown in Fig. S4. Statistical assessment of  $T_{RM}$  populations is shown. \* $p < 0.05$ , \*\* $p < 0.01$ ; one-way ANOVA test with Tukey’s multiple comparison test. (E) Representative liver sections from HBV transgenic animals with staining for HBcAg expression from animals with high or low initial viral load (shown as genomes/ml). Scale bar shows 20  $\mu$ m. (F–H) Analysis of HBcAg, CD3, or Ki67-expressing cells using Aperio imagescope software. Initial viral titres for mice shown in G and H is shown in Fig. S7. Data are expressed as mean frequency  $\pm$  SEM per treatment group. \* $p < 0.05$ , \*\* $p < 0.01$ ; one-way ANOVA test with Tukey’s multiple comparison test. CV, central vein; PV, portal vein.

were loaded with PBS-57, an analogue of  $\alpha$ -GalCer that helps forms stable tetramers that are able to bind to  $\alpha$ -GalCer-reactive cells.<sup>38</sup> Cells were washed twice in 150  $\mu$ l FACS buffer, centrifuged and the supernatant discarded, before resuspension in FACS buffer, filtered through a 70  $\mu$ m filter and analysed on a

three- or four-laser spectral flow cytometer Aurora (Cytek Biosciences) using SpectroFlo software version 2.2 and analysed using FlowJo software, version 10.7.1 (Tree Star, San Carlos, CA, USA). Gating involved exclusion of dead cells and inclusion of single cells based on FSC-A vs. FSC-H and SSC-A vs. SSC-H

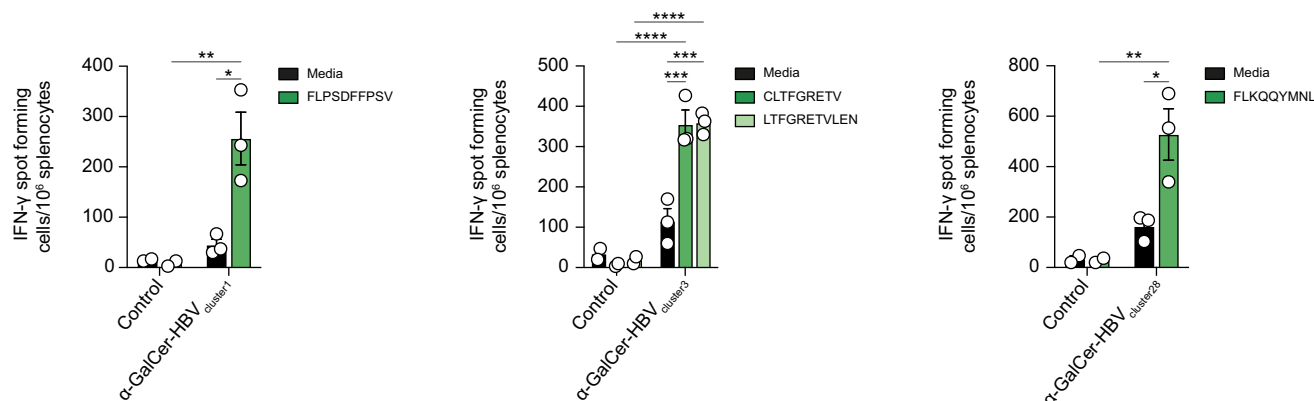


**Fig. 4. Assessment of T-cell responses to vaccines incorporating SLPs from HBV antigens in HLA-A2 mice.** Groups of HLA-A2-K<sup>b</sup> transgenic mice (n = 3) were administered vaccines prepared from synthetic long peptides (SLPs) that included HLA-A2 epitopes. Seven days later, T-cell responses to the individual HLA-A2-binding peptide(s) incorporated, were assessed by IFN- $\gamma$  ELISpot on splenocytes. Data are expressed as mean  $\pm$  SEM, with each symbol representing an individual mouse. \*p < 0.05, \*\*p < 0.01, \*\*\*p < 0.001, \*\*\*\*p < 0.0001; two-way ANOVA with Tukey's multiple comparison test.

profiles. Gating strategies for analysis of splenic antigen-presenting cells and NKT cells are provided in Figs. S2 and S3. Livers from experiments using HBV Tg  $\times$  D<sub>H</sub>LMP2a mice (and C57BL/6 controls) were processed into single cell suspensions as previously described,<sup>39,40</sup> and incubated at 37 °C for 4 h with 2  $\mu$ g/ml of Core<sub>93-100</sub> (Kb; MGLKFRQL) peptide (Primm, Italy). All flow cytometry staining of surface-expressed and intracellular molecules were performed as described.<sup>41</sup> Antibody panels are provided in Table S5, with gating strategies for intracellular cytokine staining and defining memory T cells in Figs. S4 and S5.

### Splenectomy

For splenectomy, mice were anaesthetised by i.p. injection with 100 mg/kg ketamine and 10 mg/kg xylazine, with 0.1 mg/kg buprenorphine given s.c. for analgesia (all Sigma-Aldrich). Lacrilube (Allergan New Zealand Ltd, NZ) was applied to corneas to prevent desiccation. The surgical area was sterilised with iodine, followed by an incision on the left flank and the peritoneum to access the spleen. The primary artery and vein were tied using sutures (Ethicon Prolene 7/0 Blue P1 45 cm, Amtech, Auckland, NZ), the spleen was removed, and the incision was closed by suture. Sham surgeries were performed where the peritoneum was cut and then closed by suture. Postoperative analgesia with 5 mg/kg carprofen (Norbrook Laboratories, Corby, UK) was given s.c. for 2 days post surgery.

### Assessing vaccines in transgenic model of chronic HBV infection

Male HBV Tg  $\times$  D<sub>H</sub>LMP2a mice screened to express HBeAg at  $\sim$ 200 PEI/ml and HBsAg at  $\sim$ 1,000 IU/ml at 4–5 weeks of age were used to assess antiviral activity of vaccines. On Day -1, baseline levels of serum HBeAg, HBsAg, HBV DNA and alanine aminotransferase (ALT) were determined (see below). On Day 0, groups of HBV Tg  $\times$  DHLMP2a mice (n = 8), and a C57BL/6 group (n = 6) received 10<sup>6</sup> naive HBcAg<sub>93-100</sub>-specific CD8<sup>+</sup> T cells intravenously. A control group of HBV Tg  $\times$  DHLMP2a mice (n = 8) received NaCl vehicle without transgenic T cells. On Day 1, one group of transgenic mice and the C57BL/6 group were intravenously administered the  $\alpha$ -GalCer-HBcAg<sub>93-100</sub> vaccine (3 nmol/mouse), and another group of transgenic mice were administered an equivalent molar dose of vaccine with irrelevant peptide ( $\alpha$ -GalCer-OVA<sub>257-264</sub>). The vaccinated mice received a boost at the same dose on Day 21. The

control group of mice received NaCl on days of injection. Serum samples were collected from peripheral blood on Days -1, 4, 8, 15, 22, 29, 36, 42 post HBcAg<sub>93-100</sub>-specific T<sub>N</sub> cell transfer. At Day 42 the animals were culled, and livers collected for histology and flow cytometry. Tissue sections were snap frozen in liquid nitrogen and stored at -80 °C for molecular analyses.

### Histology

For haematoxylin and eosin staining, livers were perfused with PBS, harvested in Zn-formalin and transferred into 70% ethanol 24 h later. Tissue was then processed, embedded in paraffin and stained as previously described.<sup>39</sup> Bright-field images were acquired through an Aperio Scanscope System CS2 microscope and an ImageScope program (Leica Biosystem) following the manufacturer's instructions. The antibody panel for immunohistochemistry staining is provided in Table S6. The number of HBcAg<sup>+</sup> or Ki67<sup>+</sup> hepatocytes, as well as the number of hepatic CD3<sup>+</sup> cells (expressed as % of positive cells per liver), were calculated using Aperio Imagescope software in eight separate fields (approximately 1 mm<sup>2</sup> each) from the right lateral lobe of each mouse liver. Hepatocytes were distinguished by the image analysis software based on monomorphic features, notably the almost perfect round nuclei compared with non-parenchymal cells. Results were also confirmed by manual counting.

### Analysis of viral nucleic acids

To isolate viral nucleic acids, 20  $\mu$ l of serum was incubated for 2 h at 37 °C with 180  $\mu$ l IsoHi Buffer (150 mM NaCl, 0.5% NP-40, 10 mM Tris, pH 7.4), 5 mM CaCl<sub>2</sub>, 5 mM MgCl<sub>2</sub>, 1 U DNaseI (Life Technologies, Lithuania, AM1907), and 5 U Micrococcal Nuclease (New England Biolabs, MA, USA MO247S). The digestion was stopped by the addition of 20 mM EDTA, pH 8.0, and viral nucleic acid purification was performed with the QIAmp MiniElute Virus Spin Kit (Qiagen, 57704), according to the manufacturer's instructions. Serum nucleic acids were diluted 100 times, and HBV DNA levels were quantified by real-time PCR. Reactions were performed in TaqMan Fast Universal PCR Master Mix, HBV core primers (forward TACCGCCTCAGCTCTGTATC, reverse CTTCCAAATTAACACCCACCC, probe TCACCTCACCATACTGCACTCAGGCAA). A standard curve was drawn using plasmid DNA. Reactions were run and analysed on Quant Studio 5 instrument (Life Technologies). Values for HBV DNA



were calculated as genomes/ml serum. Graphed data are expressed as fold-reduction from pretreatment levels in each animal.

### Biochemical analyses

Serum HBsAg and HBeAg were measured by ELISA (Diapro, Italy), as previously described.<sup>42,40</sup> The extent of hepatocellular injury was monitored by measuring plasma ALT activity at multiple time points after treatment, using a specialised automatic analyser (SABA PM400) as previously described.<sup>41</sup>

### Statistical analyses

Treatments were assigned to separately caged litter groups. No statistical tests were used to pre-determine sample sizes, but group sizes used are similar to those reported in previous publications.<sup>35,34</sup> Data collection and analysis were not performed blind to the conditions of the experiments. All data analysed included outliers, unless explained by technical error. Data was assumed to be normal, as the sample sizes used were not well-powered for normality testing. Figures and statistical analyses were performed using GraphPad Prism 8 software (GraphPad Prism Inc., San Diego, CA, USA).

## Results

### Conjugate vaccines stimulated NKT cells and HBV antigen-specific T cells

The small circular viral genome of HBV contains four overlapping open reading frames (ORFs) together with the regulatory elements required to control their transcription, and structural elements essential for viral replication. One ORF encodes the three forms of HBsAg that form the viral envelope (small, medium and large), whereas the other three encode: the viral HBcAg, which has an additional secreted form (HBeAg); DNA polymerase (Pol) for replication; and a non-structural protein (X) involved in transcription regulation. To demonstrate the feasibility of designing vaccines that induce targeted T-cell responses to HBV antigens through NKT cell-mediated mechanisms, we initially focussed on generating responses to HBsAg in mice. Specifically, we utilised three CD8<sup>+</sup> T-cell epitopes (HBsAg<sub>179-186</sub>, HBsAg<sub>353-360</sub>, and HBsAg<sub>371-378</sub>) that bind to H-2K<sup>b</sup>,<sup>43,44</sup> and individually conjugated these peptides to a prodrug derivative of  $\alpha$ -GalCer using a cathepsin-cleavable linker. This provided three conjugate vaccines:  $\alpha$ -GalCer-HBsAg<sub>179-186</sub>,  $\alpha$ -GalCer-HBsAg<sub>353-360</sub>, and  $\alpha$ -GalCer-HBsAg<sub>371-378</sub>. The vaccine design relied on enzymatic cleavage to release the peptide and the active form of  $\alpha$ -GalCer, which then entered the respective antigen-presenting pathways. Structures and characterisation of synthesised products are provided in the [Supplementary material](#).

Each vaccine was assessed for its capacity to stimulate peptide-specific CD8<sup>+</sup> T-cell responses in C57BL/6J mice. The animals were injected with a single i.v. dose and then 7 days later splenocytes were harvested to conduct IFN- $\gamma$  ELISpot assays after *in vitro* restimulation with each of the peptide epitopes. When compared with animals injected with vehicle as controls, significantly increased numbers of IFN- $\gamma$ -producing cells were detected in the spleens of all vaccinated mice when stimulated with relevant peptide (Fig. 1A). Further mechanistic analysis focussed on responses to the  $\alpha$ -GalCer-HBsAg<sub>371-378</sub> vaccine. Consistent with previous reports,<sup>35,45-47</sup> the importance of conjugation was confirmed by showing that injection of a mix of unconjugated components failed to induce a significant T-cell response (Fig. S1). A time-course showed that increased

numbers of peptide-specific IFN- $\gamma$ -producing cells were still detectable in the spleens 5 weeks after a single dose (Fig. 1B). Vaccination also induced responses in the liver (Fig. 1C), but the spleen was identified as the probable site of initial T-cell priming, as the liver response to  $\alpha$ -GalCer-HBsAg<sub>371-378</sub> was abrogated in splenectomised mice. Accordingly, within 18 h of vaccine administration, antigen-presenting cells in the spleen exhibited evidence of activation, with elevated expression of co-stimulatory molecules on conventional dendritic cells, and to a lesser extent, B cells (Fig. 1D). However, this activation was absent when vaccines were administered to *Traj18*<sup>-/-</sup> mice, which lack NKT cells (Fig. 1E). There was clear evidence that NKT cells were activated by the vaccines in wild-type animals, with increased NKT-cell numbers in spleen on Day 7, most showing enhanced expression of the activation marker PD-1, and a significant proportion with increased expression of KLRG-1 indicative of an effector population (Fig. 1F and Fig. S3). Consistent with previous findings following administration of NKT-cell agonists,<sup>48</sup> splenic NKT cells at Day 7 were mostly negative for NK1.1 expression and showed decreased expression of the activation marker CD69, which is typically upregulated earlier after activation but downregulated by this time point. The T-cell response to vaccination was not observed in *Traj18*<sup>-/-</sup> mice, highlighting the critical role of NKT cells in supporting cross-priming to the peptides included in the vaccine (Fig. 1G).

In translating this vaccine design to the clinic, it is important to note that NKT-cell frequency is lower in humans than in mice.<sup>20</sup> To address this difference, human CD1d-knock-in (hCD1d-KI) mice serve as a valuable model because this genetic modification results in development of a functional NKT-cell population that more closely resembles human NKT cells in terms of phenotype and frequency.<sup>28</sup> As expected, the frequency of NKT cells in the spleen of hCD1d-KI mice was ~10-fold lower than in wild-type animals (Fig. 1H). However, by 7 days after vaccination, the frequencies of NKT cells in hCD1d-KI mice were significantly increased (Fig. 1H). In fact, the population expansion was greater in hCD1d-KI mice compared with wild-type animals (~20-fold vs. twofold), resulting in similar final frequencies on the day of harvest for both strains (Fig. 1H). Importantly, despite the lower starting frequency of NKT cells in hCD1d-KI mice, a significant T-cell response to vaccination was observed, although the number of peptide-specific T-cells induced was reduced (Fig. 1I).

Overall, these findings demonstrate that the conjugate vaccine design is capable of inducing T-cell responses to defined CD8<sup>+</sup> T-cell epitopes in HBV antigens through a mechanism that also activates NKT cells—both activities could be useful in control of chronic HBV infection.

### Vaccine enhanced viral clearance in a transgenic model of chronic hepatitis B

The vaccine design was then evaluated in HBV transgenic mice. Transgenic mice of the 1.3.32 lineage express the complete HBV genome, resulting in the expression of all HBV gene products, and replication of the virus in their hepatocytes.<sup>30</sup> These mice serve as a valuable model for studying chronic HBV infection, although they do not develop symptoms of chronic hepatitis because of immunological tolerance of the viral antigens. A fraction of these transgenic mice spontaneously clear serum HBsAg by developing HBsAg-specific antibodies.<sup>26,49</sup> To assess the antiviral impact of vaccine without the interference of this antibody response, HBV transgenic animals were crossed with

D<sub>H</sub>LMP2a mice<sup>29</sup> resulting in hosts lacking surface and circulating immunoglobulins (referred to as HBV Tg × D<sub>H</sub>LMP2a mice).<sup>49</sup> Our previous studies have shown that transferring naive HBV-specific CD8<sup>+</sup> TCR transgenic T cells into 1.3.32 lineage HBV transgenic mice leads to local activation and proliferation in the liver, but failure to develop antiviral effector functions.<sup>49,31,42</sup> Therefore, this transfer model can be used to evaluate whether vaccination can induce HBV-specific T cells to exert effector functions that can control viral load. The TCR transgenic mouse strain used recognises a H-2K<sup>b</sup>-binding epitope from HBCAg antigen (HBCAg<sub>93-100</sub>), so an α-GalCer-HBCAg<sub>93-100</sub> conjugate vaccine was prepared and its capacity to induce peptide-specific immune responses was confirmed in C57BL/6J animals (Fig. 2A).

The α-GalCer-HBCAg<sub>93-100</sub> conjugate vaccine was then administered to HBV Tg × D<sub>H</sub>LMP2a mice that had been transferred with 10<sup>6</sup> naive transgenic HBCAg<sub>93-100</sub>-specific CD8<sup>+</sup> T cells (Fig. 2B). The T-cell transfer was conducted on Day 0, followed by vaccination on Days 1 and 21. A vaccine containing an irrelevant peptide epitope (α-GalCer-OVA<sub>257-264</sub>) was also tested, which was expected to induce similar levels of NKT-cell activation. A control group received NaCl vehicle without transgenic T cells, and an additional group of C57BL/6 mice was vaccinated with α-GalCer-HBCAg<sub>93-100</sub> to evaluate the impact of HBV expression on vaccine responses. Serum samples were taken from the HBV transgenic mice throughout the experiment to assess ALT, HBV DNA, HBeAg, and HBsAg levels.

The HBV Tg × D<sub>H</sub>LMP2a mice that received the conjugate vaccines exhibited a transient increase in serum ALT levels, irrespective of vaccine antigen, peaking at Day 4 (Fig. 2C). However, the α-GalCer-HBCAg<sub>93-100</sub> vaccine induced higher ALT levels that took longer to return to baseline than the irrelevant vaccine (Day 15 vs. Day 8). Both vaccines led to a decrease in serum HBsAg and HBeAg levels compared with vehicle-treated controls at Day 4 (Fig. 2D and E), suggesting that NKT-cell activation alone could contribute to controlling viral replication, as previously reported.<sup>22</sup> However, only the α-GalCer-HBCAg<sub>93-100</sub> vaccine maintained a significant reduction in these levels at later time points. Similarly, whereas both vaccines reduced serum HBV DNA levels early after vaccination compared with vehicle-treated controls (Fig. 2F), the α-GalCer-HBCAg<sub>93-100</sub> vaccine performed significantly better in reducing HBV DNA levels at later time points. A similar experiment performed in the absence of transgenic T-cell transfer failed to demonstrate superior viral control by the α-GalCer-HBCAg<sub>93-100</sub> vaccine, likely reflecting marked tolerance of endogenous T cells for viral antigens in HBV transgenic hosts (Fig. S6). The sustained activity of the virus-specific vaccine in the presence of transgenic T cells is therefore mediated via stimulation of the transferred cells.

Flow cytometry was conducted to examine the phenotype of the transgenic HBCAg<sub>93-100</sub>-specific T cells in both HBV transgenic and wild-type hosts at the end of the experiment. Interestingly, both vaccines induced the accumulation of cytokine- and granzyme B-expressing transgenic T cells in the livers of HBV transgenic animals (Fig. 3A–C). This suggests that the capacity for NKT-cell stimulation, shared by both vaccines, supported this response, potentially reflecting NKT cell-mediated licensing of the response to endogenous HBCAg protein in the host. However, a higher frequency of cytokine-producing HBCAg<sub>93-100</sub>-specific T cells was observed with the HBV-specific vaccine in wild-type animals, indicating some T-cell dysfunction in HBV transgenic hosts that could not be overcome by the vaccination strategy. A notable feature of the response to either vaccine was the

presence of a high proportion of CD44<sup>+</sup>CD69<sup>+</sup>CD62L<sup>+</sup>HBCAg<sub>93-100</sub>-specific T cells in the liver, particularly compared with the spleen, with higher levels observed in HBV transgenic hosts (Fig. 3D). This phenotype could represent T cells that have recently encountered antigens or could be associated with resident-memory cells.<sup>50</sup>

To assess whether HBV clearance could be observed histologically, liver-samples were stained for HBCAg at the end of the experiment. Comparing animals with similar initial virus titres, visible reductions in cytoplasmic HBCAg staining (an indirect marker of HBV replication)<sup>30</sup> were observed in animals that received the α-GalCer-HBCAg<sub>93-100</sub> vaccine compared with those that received the irrelevant vaccine or were untreated controls (Fig. 3E). When quantitated digitally, there was a significant reduction in the percentage of cells positive for cytoplasmic HBCAg (as a fraction of all liver cells) in the virus-specific vaccine group compared with the irrelevant vaccine and untreated control groups (Fig. 3F). Immunohistological staining also demonstrated a significant increase in CD3<sup>+</sup> cells in liver samples from α-GalCer-HBCAg<sub>93-100</sub>-vaccinated animals (Fig. 3G), as well as an increase in Ki67<sup>+</sup> cells (Fig. 3H). Proliferating hepatocytes can be identified utilising Ki67 staining and morphometric parameters, with the round shape of hepatocellular nuclei distinguishing them from the nuclei of other Ki67<sup>+</sup> non-parenchymal cells, including immune cells. Therefore, these proliferating cells may represent hepatocyte regeneration in response to vaccine-induced removal of antigen-expressing cells. Taken together with the observed decrease in viral antigens and HBV DNA levels in the serum following the α-GalCer-HBCAg<sub>93-100</sub> vaccine, these findings suggest that an advantage in antiviral activity can be achieved by including the viral peptide in the vaccine.

### Conjugate vaccines incorporating multiple HLA-restricted HBV T-cell epitopes for use in humans

To ensure comprehensive population coverage with a peptide-based vaccine for hepatitis B, it is necessary to incorporate multiple T-cell epitopes because of the high diversity of HLA alleles. This can be achieved by including several epitopes in one vaccine and/or combining different vaccines into a final product. To select suitable HBV epitopes, we conducted a review of defined HBV epitopes in patients with hepatitis B to choose a series of epitopes that would maximise population coverage based on known distribution of class I HLA alleles. It was expected that clusters of epitopes could be identified within HBV proteins that could be incorporated into SLPs of contiguous sequence. Following a query of the immune epitope database, IEDB, 86 HBV-derived HLA class I-restricted T-cell epitopes, representing 114 different HLA restrictions were identified for further analysis (Table S1). Proto-clusters of overlapping or nested sequences were identified and expanded to incorporate additional epitopes in both the N- and C-terminal directions until spans of up to approximately 32 residues were selected. In total, 35 different clusters were identified (Table 1). Using a population coverage tool hosted by the IEDB,<sup>51</sup> it was estimated that a final product containing the top eight constructs, incorporating 29 unique epitope sequences, would achieve coverage of 94.4% of individuals in the worldwide population and 97.4% of Caucasians (Table S2). On average, an individual was predicted to recognise 9.00 different epitopes in the worldwide population, or 10.08 epitopes in Caucasians. Using this information, we envisage that a final product could be prepared containing a mix of vaccines,

**Table 1. HBV epitope clusters.**

Cluster	Protein	Start pos.*	End pos.	Length	No. epitopes	Positive responses	Total tested	No. alleles†	Total coverage‡
1	HBeAg/HBcAg	47	67	21	6	184	210	10	76.1
3	HBeAg/HBcAg	117	147	31	6	20	25	5	70.3
28	Pol	665	684	20	3	12	16	4	69.9
25	Pol	531	557	27	6	34	48	5	59.0
8	HBsAg	194	223	30	3	81	88	4	57.2
13	HBsAg	343	368	26	6	114	138	4	57.1
2	HBeAg/HBcAg	89	105	17	3	15	17	2	55.0
5	HBeAg/HBcAg	170	197	28	3	24	25	4	54.7
31	Pol	—	—	—	1	4	4	2	55.0
32	X	4	34	31	3	9	16	2	55.0
17	Pol	55	69	15	2	5	10	3	47.7
12	HBsAg	324	343	20	3	10	13	4	43.5
14	HBsAg	367	390	24	5	23	27	3	41.4
4	HBeAg/HBcAg	146	156	11	2	16	23	2	35.8
9	HBsAg	245	256	12	2	7	10	2	35.8
27	Pol	651	661	11	2	7	15	2	33.8
29	Pol	756	784	29	2	13	22	1	31.9
18	Pol	94	102	9	1	5	7	1	31.9
23	Pol	453	461	9	1	30	36	2	29.6
26	Pol	573	581	9	1	26	34	1	28.5
34	X	92	123	32	2	20	26	1	28.5
10	HBsAg	261	280	20	4	19	25	1	28.5
30	Pol	814	822	9	1	18	21	1	28.5
7	HBsAg	182	196	15	2	8	10	2	28.5
24	Pol	500	510	11	2	7	11	1	28.5
33	X	52	60	9	1	7	12	1	28.5
35	X	140	148	9	1	5	6	1	28.5
6	HBsAg	74	95	22	2	4	4	1	28.5
15	HBsAg	—	—	—	1	3	3	1	28.5
16	HBsAg	—	—	—	1	3	3	1	28.5
22	Pol	422	430	9	1	2	6	1	28.5
19	Pol	149	175	27	3	9	15	3	27.1
20	Pol	365	374	10	1	4	6	3	24.1
21	Pol	388	397	10	2	8	12	2	20.2
11	HBsAg	306	315	10	1	4	4	1	15.8

The top eight clusters for population coverage are shown above the line. A dash indicates that the epitope did not align with the corresponding HBV reference sequence.  
 \* Starting position indexed to the corresponding reference sequences: POC767, HBeAg inclusive of HBcAg; Q76R62, large HBsAg; Q69028, Pol.  
 † Number of unique restricting HLA alleles.  
 ‡ Clusters are ordered based on population coverage for known distribution of HLA alleles worldwide, which is defined as the geographic regions: Europe, North Africa, North-East Asia, the South Pacific (Australia and Oceania), Hispanic North and South America, American Indian, South-East Asia, South-West Asia, Sub-Saharan Africa. Pol, DNA polymerase; HLA, human leukocyte antigen.

each based on a different cluster. To limit the number of vaccines needed, and thereby reduce manufacturing costs, coverage by just three clusters was considered: cluster 1, which contained the well-characterised HBcAg<sub>47-58</sub> epitope (also commonly termed HBcAg<sub>18-27</sub>), and clusters 3 and 28, from HBcAg and Pol, respectively, which both had strong overall coverage. In choosing these candidates for further evaluation, two further considerations were made. First, it was established that extending the N-terminus of cluster 1 by two amino acids of sequence incorporated a known MHC class II-binding CD4<sup>+</sup> T-cell epitope, as did a C-terminal extension of one amino acid to cluster 3. Second, sequence adaptations were made to account for common variants, resulting in minor modifications to clusters 1 and 28. The inclusion of these variant sequences in the subsequent population coverage analysis led to a lower number of evaluated epitopes for some clusters compared with Table 1. Nonetheless, a combination of just these three clusters, containing 12 unique epitopes, was predicted to provide coverage of 91.9% of individuals in the worldwide population, and 95.9% of Caucasians, with the average individual recognising 3.38 and 3.94 different epitopes, respectively (Table 2).

To assess whether individual epitopes could be effectively processed and presented from vaccines prepared with SLPs,

immunogenicity studies were conducted in HLA-A2 transgenic mice. Individual vaccines were prepared using SLPs encompassing clusters 1, 3 and 28 ( $\alpha$ -GalCer-HBV<sub>cluster1</sub>,  $\alpha$ -GalCer-HBV<sub>cluster3</sub>, and  $\alpha$ -GalCer-HBV<sub>cluster28</sub>), and each was tested for capacity to stimulate peptide-specific CD8<sup>+</sup> T-cell responses after a single i.v. dose. All three vaccines induced responses to HLA-A2-binding peptides contained within the SLPs used in their manufacture (Fig. 4).

## Discussion

In this study, we describe the construction of peptide-glycolipid conjugate vaccines that recruit the licencing capacity of NKT cells to support HBV-specific CD8<sup>+</sup> T-cell responses with antiviral activity. The vaccines are composed of peptides encompassing known CD8<sup>+</sup> T-cell epitopes from HBV antigens that have been synthetically conjugated to a derivative of  $\alpha$ -GalCer. Following i.v. administration, a route chosen to maximise access to NKT cell-rich tissues, antigen-presenting cells were activated through the licencing activity of NKT cells, with the spleen being a major site of T-cell priming. Although the mechanism is reliant on NKT-cell function, human CD1d knock-in mice with low resting frequencies of NKT cells that approximate levels

**Table 2. Population coverage of consensus sequence cluster constructs.**

Construct	Sequence	Epitopes (n)	Worldwide		Caucasians	
			Population coverage	Avg. epitope/HLA*	Population coverage	Avg. epitope/HLA
Cluster 1	<b>LS</b> FLPSDFP <b>SV</b> RLLD <b>TAS</b> ALY	4	68.1%	1.15	79.4%	1.52
Cluster 3	YVNTNMGLKILQLLWFHISCLTFGRET <b>VLEN</b>	6	71.7%	1.30	72.8%	1.41
Cluster 28	QA <b>FT</b> FSPTYKA <b>FLKQ</b> QY <b>MNL</b>	2	75.2%	0.93	80.2%	1.01
Clusters 1, 3 and 28		12	91.9%	3.38	95.9%	3.94

Amino acids in bold denote changes from original cluster sequences in Table S2 as specified in text.

\* Average number of epitope/HLA combinations recognised by individuals in the population.

seen in humans were still capable of inducing significant T-cell responses. To test the antiviral activity of the vaccine platform, a conjugate incorporating the H-2K<sup>b</sup>-binding CD8<sup>+</sup> T-cell epitope HBCAg<sub>93-100</sub> was evaluated in HBV transgenic animals. While it has previously been reported that transfer of naive HBCAg<sub>93-100</sub>-specific CD8<sup>+</sup> TCR transgenic T cells into HBV transgenic hosts leads to local proliferation in the liver, but failure to develop antiviral effector functions,<sup>31,42</sup> here we found that vaccination after transfer was associated with measurable antiviral activity. This was characterised by reduced levels of HBsAg, HBeAg, and HBV DNA in serum and reduced HBCAg expression in the liver, with the transgenic T cells retaining capacity for cytokine production by the end of the experiment (Day 43), albeit reduced compared with transfer and vaccination in HBV-negative hosts. We also noted evidence of cellular proliferation in liver sections that was potentially indicative of liver regeneration in response to vaccine-induced removal of virus-infected cells.

The vaccine-stimulated T cells in HBV transgenic animals retained some capacity for cytokine production, and expressed granzyme B. However, these measured attributes cannot be the full explanation for the antiviral response observed with the HBV-specific vaccine, as administration of a similar vaccine construct with an irrelevant peptide ( $\alpha$ -GalCer-OVA<sub>257-264</sub>) induced comparable expansion of the transgenic T-cell population, with a similar broad range of memory phenotypes, and also some antiviral activity. As both vaccines shared the NKT agonist, it is possible that NKT cell-mediated licensing of APCs that had acquired endogenous HBCAg protein from the HBV transgenic hosts played a dominant role in shaping this T-cell response profile. Both vaccines induced accumulation of CD44<sup>+</sup> CD62L<sup>-</sup> transgenic T cells expressing CD69 in the liver, which could indicate recent antigen exposure or potentially the presence of liver resident memory T cells (T<sub>RM</sub>).<sup>50</sup> To confirm the induction of *bona fide* liver T<sub>RM</sub> would require further assessment to show enhanced expression of other defining markers, such CXCR6, and ultimately require studies to prove long-term residency. However, we have previously shown that similar conjugate vaccines are highly effective at inducing T<sub>RM</sub> after i.v. administration to wild-type hosts,<sup>46</sup> suggesting that the activation of liver-resident NKT cells can create a favourable local inflammatory environment for T<sub>RM</sub> recruitment and residency. In the current study, greater numbers of CD69<sup>+</sup> T cells were observed in the liver after vaccination of HBV transgenic hosts compared with C57BL/6 hosts, suggesting the presence of endogenous HBV antigens contributed to accumulation of these cells. Indeed, both local inflammation and antigen expression have previously been identified as strong contributing factors to liver T<sub>RM</sub> accumulation in other models.<sup>50,52</sup> Although liver T<sub>RM</sub> have been associated with the control of HBV,<sup>53</sup> the superior activity of the HBV-specific vaccine in our study was not associated with increased

accumulation of CD69<sup>+</sup> cells in the liver when compared with the irrelevant vaccine, although it is possible that the proportion of *bona fide* T<sub>RM</sub> within this population may have been higher. Therefore, the specific advantageous characteristic induced by direct vaccine-induced stimulation of the transgenic cells using the HBV-specific vaccine remains undefined. It is plausible that a bias for vaccine-derived peptide to be presented by professional APCs may have driven such a qualitatively improved response. The requirement for cathepsin-mediated cleavage of the vaccine before presentation may have contributed to this, as professional APCs tend to exhibit enhanced cathepsin activity.<sup>54</sup>

We anticipate that activated NKT cells may have contributed to the antiviral effects of both vaccines, potentially through the production of antiviral cytokines such as IFN- $\gamma$ .<sup>22</sup> However, because of the significant adjuvant effect on the T-cell response (even with the irrelevant vaccine), it was not possible to specifically dissect the direct antiviral contribution of these cells. In the study of Kakimi *et al.*,<sup>22</sup> administration of just 10 ng of  $\alpha$ -GalCer was sufficient to induce an NKT cell-mediated reduction in HBV replication in HBV transgenic mice for at least 7 days. It is difficult to directly compare this previously reported response to the magnitude and quality of the NKT-cell response observed with the conjugate vaccines, as this would depend on the rate of enzymatic release of  $\alpha$ -GalCer from the conjugate structure. Our studies based on similar conjugate designs have shown that the profile of cytokine release following administration is altered when compared with administration of unconjugated  $\alpha$ -GalCer. In particular, we observed a smaller percentage of NKT cells releasing IL-4 and IFN- $\gamma$  (with reduced cytokine production per cell), whereas induction of IL-12p70 by licenced antigen-presenting cells and IFN- $\gamma$  production through transactivation of NK cells remained similar.<sup>34</sup> Therefore, conjugation appears to induce the licensing activity of NKT cells despite a generally weaker NKT-cell response, likely because of a preference for the conjugate to be processed in professional antigen-presenting cells, such as the cDC1 subset primarily responsible for IL-12p70 production.<sup>55,56</sup>

To achieve comprehensive population coverage with a peptide-based vaccine format in the human population, it was necessary to design HBV vaccines that incorporate several T-cell epitopes to account for high HLA diversity. Through a review of defined HBV epitopes in HBV patients, we identified a series of epitope clusters that were incorporated into SLPs. Based on the known HLA distribution worldwide, a combination of the top three cluster SLPs was predicted to give 91.9% coverage, with an average of 3.38 epitopes recognised per individual. These numbers may be conservative because they are based on epitope discovery data that are biased towards Caucasians. It is likely that several of the epitopes will also serve as *bona fide* epitopes in closely related HLA variants that are common in different ethnicities, although this has not been directly tested. Importantly,

the immunogenicity studies conducted here using HLA-A2 transgenic mice confirmed the capacity of vaccines incorporating SLPs to induce peptide-specific T-cell responses *in vivo*, indicating that the peptides can be acquired, processed, and presented from the longer peptide format.

Clinical evaluation of  $\alpha$ -GalCer as a standalone treatment in chronic hepatitis B resulted in only a transient decrease in HBV DNA in three of 21 patients. Furthermore, four patients discontinued treatment because of fever.<sup>57</sup> It remains to be established what impact the conjugation of peptide to introduce an additional CD8<sup>+</sup> T-cell-mediated effector arm would have on both efficacy and safety in patients. We have evidence that conjugation is dose-sparing in terms of peptide levels required to induce antitumour CD8<sup>+</sup> T-cell responses in mice,<sup>35</sup> meaning it may be possible to find a dose that balances effective T-cell activity with reduced NKT-cell activity and a good safety profile. We have also shown that it is possible to reduce liver inflammation by decreasing the acyl chain length on the NKT-cell agonist used for conjugation.<sup>46</sup> Others have shown that

encapsulating NKT-cell agonists into nanoparticles improves the safety profile,<sup>58</sup> which may be possible to achieve by incorporating our vaccines into lipid-based particles. It is also worth noting that the use of SLPs to elicit T-cell responses in patients with chronic hepatitis B has been explored by others, with a series of HBV-derived SLPs shown to induce IFN- $\gamma$  responses in *ex vivo* stimulated peripheral blood mononuclear cells from chronic patients,<sup>59–61</sup> and a clinical trial of SLPs vs. placebo is now currently recruiting patients (NCT05841095).

In summary, the conjugate vaccine design described here successfully elicited virus-specific T cells exerting antiviral activity in a model of chronic hepatitis B. Through a stringent epitope selection process and the assembly of clustered epitopes into regions of contiguous sequence of manageable peptide size for conjugation, three vaccines have been identified as potential candidates for further clinical evaluation as a combined product with good population coverage for the treatment of chronic hepatitis B.

## Abbreviations

ALT, alanine aminotransferase; AoAA, aminoxyacetic acid; DCs, dendritic cells; HLA, human leukocyte antigen; IEDB, Immune Epitope Database; IFN, interferon; mAb, monoclonal antibody; MAIT, mucosal-associated invariant T; MHC, major histocompatibility complex; NKT, natural killer T cell; Pol, HBV DNA polymerase; RBCs, red blood cells; RT, room temperature; SLPs, synthetic long peptides; TCR, T-cell receptor;  $\alpha$ -GalCer,  $\alpha$ -Galactosylceramide.

## Financial support

This work was supported with funding from the New Zealand Ministry of Business Innovation and Employment (RTVU1603), the Independent Research Organisation Fund of the Health Research Council of New Zealand to the Malaghan Institute (HRC14/1003), Callaghan Innovation R&D Project Grant (CONT-59888-PROJECT AIMMU) and Avalia Immunotherapies Limited. SAG was supported by Avalia Immunotherapies Limited. DIG was supported by an NHMRC SPRF fellowship (1117766) and now by an NHMRC Investigator grant (2008913).

## Conflict of interest

None of the authors have any conflict of interest. Please refer to the accompanying ICMJE disclosure forms for further details.

## Author contributions

Designed and synthesised the conjugate vaccines: GFP, SLD, RAJ, BJC. Assessed activity of the conjugates *in vivo*, except in HBV transgenic mice: IFH, AHM, OKB, CT, KJF. Prepared and supplied hCD1d-KI mice: WY. Conceived experiments in HBV mice and evaluated results: MI, LGG, FVC, IFH, GFP, SAG, DIG, WRH, AS. Conducted experiments in HBV transgenic mice. MI, LGG, PDL, MR, VF, LG, EB. Conceived design of peptides for wide population coverage: AS, SAG, FVC, IFH, GFP. Designed peptides based on defined epitopes in patients: AS, JS. Wrote the manuscript IFH, OKB, AHM. Contributed to reviewing and editing the manuscript: all authors.

## Data availability statement

The data that support the findings of this study are available from the corresponding author, IFH, upon request.

## Acknowledgements

We thank the personnel of the Biomedical Research Unit of the Malaghan Institute of Medical Research for animal husbandry and the Hugh Green Cytometry Centre for support with flow cytometry. We thank the NIH

tetramer Core facility for the PBS-57-loaded CD1d tetramers, and Germaine Uys for assistance with splenectomy surgery.

## Supplementary data

Supplementary data associated with this article can be found, in the online version, at <https://doi.org/10.1016/j.jhepr.2024.101038>.

## References

*Author names in bold designate shared co-first authorship*

- [1] Yuen MF, Chen DS, Dusheiko GM, et al. Hepatitis B virus infection. *Nat Rev Dis Primers* 2018;4:18035.
- [2] Iannacone M, Guidotti LG. Immunobiology and pathogenesis of hepatitis B virus infection. *Nat Rev Immunol* 2022;22:19–32.
- [3] Liaw YF, Sung JY, Chow WC, et al. Lamivudine for patients with chronic hepatitis B and advanced liver disease. *N Engl J Med* 2004;351:1521–1531.
- [4] Lau GKK, Piratvisuth T, Luo KX, et al. Peginterferon Alfa-2a, lamivudine, and the combination for HBeAg-positive chronic hepatitis B. *N Engl J Med* 2005;352:2682–2695.
- [5] Odenwald MA, Paul S. Viral hepatitis: past, present, and future. *World J Gastroenterol* 2022;28:1405–1429.
- [6] Thomas DL. Global elimination of chronic hepatitis. *N Engl J Med* 2019;380:2041–2050.
- [7] World Health Organization. Global health sector strategies on, respectively, HIV, viral hepatitis and sexually transmitted infections for the period 2022–2030. Geneva: WHO; 2022; <https://iris.who.int/bitstream/handle/10665/360348/9789240053779-eng.pdf?sequence=1>. Assessed October 2023.
- [8] Thimme R, Wieland S, Steiger C, et al. CD8<sup>+</sup> T cells mediate viral clearance and disease pathogenesis during acute hepatitis B virus infection. *J Virol* 2003;77:68–76.
- [9] Lok AS, Liang RH, Chung HT. Recovery from chronic hepatitis B. *Ann Intern Med* 1992;116:957–958.
- [10] Ilan Y, Nagler A, Adler R, et al. Ablation of persistent hepatitis B by bone marrow transplantation from a hepatitis B-immune donor. *Gastroenterology* 1993;104:1818–1821.
- [11] Lau GKK, Lok ASF, Liang RHS, et al. Clearance of hepatitis B surface antigen after bone marrow transplantation: role of adoptive immunity transfer. *Hepatology* 1997;25:1497–1501.
- [12] Loggi E, Bihl F, Chisholm JV, et al. Anti-HBs re-seroconversion after liver transplantation in a patient with past HBV infection receiving a HBsAg positive graft. *J Hepatol* 2009;50:625–630.
- [13] Penna A, Chisari FV, Bertolotti A, et al. Cytotoxic T lymphocytes recognize an HLA-A2-restricted epitope within the hepatitis B virus nucleocapsid antigen. *J Exp Med* 1991;174:1565–1570.
- [14] Asabe S, Wieland SF, Chattopadhyay PK, et al. The size of the viral inoculum contributes to the outcome of hepatitis B virus infection. *J Virol* 2009;83:9652–9662.

- [15] Yang PL, Althage A, Chung J, et al. Immune effectors required for hepatitis B virus clearance. *Proc Natl Acad Sci U S A* 2010;107:798–802.
- [16] Wang X, Dong Q, Li Q, et al. Dysregulated response of follicular helper T cells to hepatitis B surface antigen promotes HBV persistence in mice and associates with outcomes of patients. *Gastroenterology* 2018;154:2222–2236.
- [17] Cargill T, Barnes E. Therapeutic vaccination for treatment of chronic hepatitis B. *Clin Exp Immunol* 2021;205:106–118.
- [18] Tay SS, Wong YC, McDonald DM, et al. Antigen expression level threshold tunes the fate of CD8 T cells during primary hepatic immune responses. *Proc Natl Acad Sci USA* 2014;111:E2540–E2549.
- [19] Fiscaro P, Barili V, Rossi M, et al. Pathogenetic mechanisms of T cell dysfunction in chronic HBV infection and related therapeutic approaches. *Front Immunol* 2020;11:849.
- [20] Godfrey DI, Uldrich AP, McCluskey J, et al. The burgeoning family of unconventional T cells. *Nat Immunol* 2015;16:1114–1123.
- [21] Brennan PJ, Brigl M, Brenner MB. Invariant natural killer T cells: an innate activation scheme linked to diverse effector functions. *Nat Rev Immunol* 2013;13:101–117.
- [22] Kakimi K, Guidotti LG, Koezuka Y, et al. Natural killer T cell activation inhibits hepatitis B virus replication in vivo. *J Exp Med* 2000;192:921–930.
- [23] Morita M, Motoki K, Akimoto K, et al. Structure-activity relationship of  $\alpha$ -galactosylceramides against B16-bearing mice. *J Med Chem* 1995;38:2176–2187.
- [24] Schneiders FL, Scheper RJ, von Blomberg BME, et al. Clinical experience with  $\alpha$ -galactosylceramide (KRN7000) in patients with advanced cancer and chronic hepatitis B/C infection. *Clin Immunol* 2011;140:130–141.
- [25] Cerundolo V, Silk JD, Masri SH, et al. Harnessing invariant NKT cells in vaccination strategies. *Nat Rev Immunol* 2009;9:28–38.
- [26] Chandra S, Zhao M, Budelsky A, et al. A new mouse strain for the analysis of invariant NKT cell function. *Nat Immunol* 2015;16:799–800.
- [27] Serody JS, Collins EJ, Tisch RM, et al. T cell activity after dendritic cell vaccination is dependent on both the type of antigen and the mode of delivery. *J Immunol* 2000;164:4961–4967.
- [28] Wen X, Rao P, Carreño LJ, et al. Human CD1d knock-in mouse model demonstrates potent antitumor potential of human CD1d-restricted invariant natural killer T cells. *Proc Natl Acad Sci U S A* 2013;110:2963–2968.
- [29] Casola S, Otipoby KL, Alimzhanov M, et al. B cell receptor signal strength determines B cell fate. *Nat Immunol* 2004;5:317–327.
- [30] Guidotti LG, Matzke B, Schaller H, et al. High-level hepatitis B virus replication in transgenic mice. *J Virol* 1995;69:6158–6169.
- [31] Isogawa M, Chung J, Murata Y, et al. CD40 activation rescues antiviral CD8<sup>+</sup> T cells from PD-1-mediated exhaustion. *Plos Pathog* 2013;9:e1003490.
- [32] Lee A, Farrand KJ, Dickgreber N, et al. Novel synthesis of  $\alpha$ -galactosylceramides and confirmation of their powerful NKT cell agonist activity. *Carbohydr Res* 2006;341:2785–2798.
- [33] Giaccone G, Punt CJA, Ando Y, et al. A phase I study of the natural killer T-cell ligand alpha-galactosylceramide (KRN7000) in patients with solid tumors. *Clin Cancer Res* 2002;8:3702–3709.
- [34] Anderson RJ, Tang CW, Daniels NJ, et al. A self-adjuvanting vaccine induces cytotoxic T lymphocytes that suppress allergy. *Nat Chem Biol* 2014;10:943–949.
- [35] Anderson RJ, Compton BJ, Tang CW, et al. NKT cell-dependent glycolipid-peptide vaccines with potent anti-tumour activity. *Chem Sci* 2015;6:5120–5127.
- [36] Flechtner JB, Cohane KP, Mehta S, et al. High-affinity interactions between peptides and heat shock protein 70 augment CD8<sup>+</sup> T lymphocyte immune responses. *J Immunol* 2006;177:1017–1027.
- [37] Malyala P, Singh M. Endotoxin limits in formulations for preclinical research. *J Pharm Sci* 2008;97:2041–2044.
- [38] Liu Y, Goff RD, Zhou D, et al. A modified alpha-galactosyl ceramide for staining and stimulating natural killer T cells. *J Immunol Methods* 2006;312:34–39.
- [39] Iannacone M, Sitia G, Isogawa M, et al. Platelets mediate cytotoxic T lymphocyte-induced liver damage. *Nat Med* 2005;11:1167–1169.
- [40] Tontí E, Jiménez de Oya N, Galliverti G, et al. Bisphosphonates target B cells to enhance humoral immune responses. *Cell Rep* 2013;5:323–330.
- [41] Guidotti LG, Inverso D, Sironi L, et al. Immunosurveillance of the liver by intravascular effector CD8<sup>+</sup> T cells. *Cell* 2015;161:486–500.
- [42] Bénéchet AP, De Simone G, Di Lucia P, et al. Dynamics and genomic landscape of CD8<sup>+</sup> T cells undergoing hepatic priming. *Nature* 2019;574:200–205.
- [43] Lau LS, Fernandez Ruiz D, Davey GM, et al. Blood-stage *Plasmodium berghei* infection generates a potent, specific CD8<sup>+</sup> T-cell response despite residence largely in cells lacking MHC I processing machinery. *J Infect Dis* 2011;204:1989–1996.
- [44] Vita R, Mahajan S, Overton JA, et al. The immune epitope database (IEDB): 2018 update. *Nucleic Acids Res* 2019;47:D339–D343.
- [45] Speir M, Authier-Hall A, Brooks CR, et al. Glycolipid-peptide conjugate vaccines enhance CD8<sup>+</sup> T cell responses against human viral proteins. *Sci Rep* 2017;7:1–12.
- [46] Holz LE, Chua YC, de Menezes MN, et al. Glycolipid-peptide vaccination induces liver-resident memory CD8<sup>+</sup> T cells that protect against rodent malaria. *Sci Immunol* 2020;5:1–13.
- [47] Burn OK, Farrand K, Pritchard T, et al. Glycolipid-peptide conjugate vaccines elicit CD8<sup>+</sup> T-cell responses and prevent breast cancer metastasis. *Clin Transl Immunol* 2022;11:e1401.
- [48] Wilson MT, Johansson C, Olivares-Villagómez D, et al. The response of natural killer T cells to glycolipid antigens is characterized by surface receptor down-modulation and expansion. *Proc Natl Acad Sci U S A* 2003;100:10913–10918.
- [49] Fumagalli V, Di Lucia P, Venzin V, et al. Serum HBsAg clearance has minimal impact on CD8<sup>+</sup> T cell responses in mouse models of HBV infection. *J Exp Med* 2020;217.
- [50] Ghilas S, Valencia-Hernandez AM, Enders MH, et al. Resident memory T cells and their role within the liver. *Int J Mol Sci* 2020;21:1–15.
- [51] Bui HH, Sidney J, Dinh K, et al. Predicting population coverage of T-cell epitope-based diagnostics and vaccines. *BMC Bioinformatics* 2006;7:153.
- [52] Fernandez-Ruiz D, Ng WY, Holz LE, et al. Liver-resident memory CD8<sup>+</sup> T cells form a front-line defense against malaria liver-stage infection. *Immunity* 2016;51:889–902.
- [53] Pallett LJ, Davies J, Colbeck EJ, et al. IL-2high tissue-resident T cells in the human liver: sentinels for hepatotropic infection. *J Exp Med* 2017;214:1567–1580.
- [54] Watts C. Capture and processing of exogenous antigens for presentation on MHC molecules. *Annu Rev Immunol* 1997;15:821–850.
- [55] Kitamura H, Iwakabe K, Yahata T, et al. The natural killer T (NKT) cell ligand alpha-galactosylceramide demonstrates its immunopotentiating effect by inducing interleukin (IL)-12 production by dendritic cells and IL-12 receptor expression on NKT cells. *J Exp Med* 1999;189:1121–1128.
- [56] Farrand KJ, Dickgreber N, Stoitzner P, et al. Langerin<sup>+</sup> CD8 $\alpha^+$  dendritic cells are critical for cross-priming and IL-12 production in response to systemic antigens. *J Immunol* 2009;183:7732–7742.
- [57] Woltman AM, Ter Borg MJ, Binda RS, et al.  $\alpha$ -Galactosylceramide in chronic hepatitis B infection: results from a randomized placebo-controlled Phase I/II trial. *Antivir Ther* 2009;14:809–818.
- [58] Tefit JN, Crabé S, Orlandini B, et al. Efficacy of ABX196, a new NKT agonist, in prophylactic human vaccination. *Vaccine* 2014;32:6138–6145.
- [59] Dou Y, van Montfoort N, van den Bosch A, et al. HBV-derived synthetic long peptide can boost CD4<sup>+</sup> and CD8<sup>+</sup> T-cell responses in chronic HBV patients ex vivo. *J Infect Dis* 2018;217:827–839.
- [60] Dou Y, Jansen DTSL, van den Bosch A, et al. Design of TLR2-ligand-synthetic long peptide conjugates for therapeutic vaccination of chronic HBV patients. *Antivir Res* 2020;178:104746.
- [61] Jansen DTSL, de Beijer MTA, Luijten RJ, et al. Induction of broad multi-functional CD8<sup>+</sup> and CD4<sup>+</sup> T cells by hepatitis B virus antigen-based synthetic long peptides ex vivo. *Front Immunol* 2023;14.